

## QUASAR X-RAY SPECTRA REVISITED<sup>1</sup>

P. SHASTRI,<sup>2,3</sup> B. J. WILKES,<sup>4</sup> M. ELVIS,<sup>4</sup> AND J. MCDOWELL<sup>4</sup>

Received 1992 May 6; accepted 1992 November 30

### ABSTRACT

A sample of 45 quasars observed by the IPC on the *Einstein* satellite is used to reexamine the relationship of the soft (0.2–3.5 keV) X-ray energy index with radio properties and the optical Fe II emission. We find that (1) the tendency for radio-loud quasars to have systematically flatter X-ray energy indices than radio-quiet quasars is confirmed with the soft X-ray excess having negligible effect; (2) there is a tendency for the flatness of the X-ray slope to correlate with radio core dominance for radio-loud quasars, suggesting that a component of the X-ray emission is relativistically beamed; (3) for the radio-quiet quasars, the soft X-ray energy indices with a mean of  $\sim 1.0$  are consistent with the indices found at higher energies (2–10 keV), although steeper than those observed for Seyfert 1 galaxies (also 2–10 keV) where the reflection model gives a good fit to the data; (4) the correlation of Fe II emission line strength with X-ray energy index is confirmed for radio-quiet quasars using a subset of 18 objects. The radio-loud quasars show no evidence for a correlation. This relation suggests a connection between the ionizing continuum and line emission from the broad emission-line region (BELR) of radio-quiet quasars, but in the opposite sense to that predicted by current photoionization models; (5) the correlations of X-ray slope with radio core dominance and Fe II equivalent width within the radio-loud and radio-quiet subclasses, respectively, imply that the observed wide range of X-ray energy indices is real rather than due to the large measuring uncertainties for individual objects.

*Subject headings:* galaxies: active — quasars: emission lines — quasars: general — radio continuum: galaxies — X-rays: galaxies

### 1. INTRODUCTION

The powerful X-ray emission that is commonly seen from quasars and other active galactic nuclei is widely believed to originate close to the “central engine” in these objects. Recent studies have made it clear that there is a wide range in the energy indices of the X-ray emission, both in the soft ( $\sim 0.3$ – $2$  keV: Wilkes & Elvis 1987) and hard (2–10 keV: Comastri et al. 1992; Williams et al. 1992) energy ranges, laying to rest the older view that X-ray energy indices of all broad-line active galactic nuclei can be adequately described by a single power law of slope  $\sim 0.7$  (e.g., Mushotzky 1984). The details of the X-ray emission mechanisms in different types of quasars, however, are not well understood.

Wilkes & Elvis (1987) derived X-ray energy indices,  $\alpha_E$  ( $f_\nu \sim \nu^{-\alpha_E}$ ), in the soft X-ray region (0.2–3.5 keV) for a sample of 33 quasars that were observed with sufficient signal-to-noise with the *Einstein* IPC. They reported that the best-fit power-law energy indices have a wide range ( $-0.2$  to  $1.8$ ), and that radio-loudness correlated with the soft X-ray energy index in the sense that radio-loud quasars (RLQs) had flatter X-ray energy indices than radio-quiet quasars (RQQs). They argued for a two-component model for the X-ray emission: one linked to the radio emission and of somewhat flatter slope ( $\sim 0.5$ ); and the second of steeper slope ( $\sim 1$ ) that was ubiquitous in quasars. Wilkes & Elvis (1987) explained the difference between these soft energy indices and the mean energy index of  $\sim 0.7$  observed at higher energies in terms of a mixing of the two components. They also found evidence for an upturn in

the X-ray spectrum at lower energies (less than 0.3 keV)—the “ultrasoft excess”—as discovered by *EXOSAT* (Arnaud et al. 1985).

Here we study the behavior of the X-ray energy indices of quasars with an enlarged sample of 45 objects using new IPC spectral fits from the atlas of quasar energy distributions (Elvis et al. 1993). The spectral fits were obtained by fitting a power-law to the X-ray energy distribution, allowing both the power-law index and the equivalent hydrogen column density of absorbing cold matter to be free parameters as in Wilkes & Elvis (1987). When required by the ultrasoft excess, we use updated X-ray energy indices from Masnou et al. (1992), which have been determined with a broken power-law that properly accounts for this excess. We reexamine the connection with radio-loudness (Wilkes & Elvis 1987) and with the radio core-dominance parameter (Shastri 1991), and also consider a possible relation between X-ray slope and the strength of the Fe II (optical) emission lines suggested by Wilkes, Elvis, & McHardy (1987) but later questioned by Boroson (1989) and Zheng & O’Brien (1990).

### 2. RADIO-LOUD AND RADIO-QUIET QUASARS

Here we use the radio-loudness parameter ( $R_L$ ) to distinguish between quasars that do exhibit the phenomenon of powerful radio jets and those that do not (cf. Wilkes & Elvis 1987). We define radio-loudness ( $R_L$ ) as  $\log(f_R/f_B)$ , where  $f_R$  and  $f_B$  are the flux densities (in mJy) in the 5 GHz and  $B$  bands, respectively (cf. Kellermann et al. 1989). The flux density  $f_B$  is calculated from the  $B$ -magnitude (Hewitt & Burbidge 1987 or Veron-Cetty & Veron 1991) using  $m_B(0) = 4440$  Jy (Johnson 1966). When  $B$ -magnitudes were not available,  $V$ -magnitudes were used. References for the 5 GHz flux densities of the RQQs are listed in Table 1. For the RLQs, they were taken from Kühr et al. (1979) or Veron-Cetty & Veron (1991). Note that the definition differs from the one adopted by Wilkes & Elvis

<sup>1</sup> Based in part on data acquired at the Multiple Mirror Telescope (MMT), a joint facility of the Smithsonian Institution and the University of Arizona.

<sup>2</sup> Department of Astronomy, University of Texas, Austin, TX 78712.

<sup>3</sup> Present address: Astronomy Department, 601 Campbell Hall, University of California, Berkeley, CA 94720.

<sup>4</sup> Harvard-Smithsonian Center for Astrophysics, 60 Garden Street, Cambridge MA 02138.

TABLE 1  
RADIO-QUIET QUASARS

| Source                | Other Name   | Redshift | $f_B^a$<br>(mJy) | $R_{L_i}$    | $\alpha_E$<br>( $\pm 1 \sigma$ ) | Reference <sup>b</sup> | Reference <sup>c</sup><br>( $\alpha_E$ ) | $W_\lambda^d$<br>(Å) | Reference <sup>c</sup><br>( $W_\lambda$ ) | FWHM <sup>e</sup><br>(km s <sup>-1</sup> ) |
|-----------------------|--------------|----------|------------------|--------------|----------------------------------|------------------------|--|----------------------|---|--|
| 0026+129              | PG           | 0.142    | 2.33             | 0.34         | $0.88_{-0.05}^{+0.05}$           | 1                      | 4  |                      |   |  |
| 0054+144              | PHL 909      | 0.171    | 1.0              | -0.01        | $0.41_{-0.07}^{+0.07}$           | 2                      | 4  |                      |   |  |
| 0205+024              | NAB          | 0.155    | 2.25             | -0.18        | $1.2_{-0.07}^{+0.07}$            | 3                      | 4  |                      |   |  |
| 0844+349 <sup>f</sup> | PG           | 0.064    | 11.2             | -1.56        | $1.6_{-0.7}^{+0.7}$              | 1                      | 2  | 46                   | 1, 2                                      | 3380                                       |
| 0923+129 <sup>f</sup> | PG           | 0.028    | 4.74             | 0.32         | $0.7_{-0.3}^{+0.3}$              | 1                      | 2  | 29                   | 2   | 1840                                       |
| 1116+215              | PG           | 0.177    | 3.80             | -0.13        | $1.0_{-0.2}^{+0.2}$              | 1                      | 3  | 15                   | 1   | 4290                                       |
| 1202+281              | GQ Comae     | 0.165    | 2.33             | -0.45        | $1.1_{-0.4}^{+0.2}$              | 1                      | 3, 6                                     |                      |   |  |
| 1211+143              | PG           | 0.085    | 6.24             | 0.89         | $1.8_{-0.2}^{+0.4}$              | 4                      | 3  | 32*                  | 1, 2                                      | 3000                                       |
| 1219+755              | Mkn 205      | 0.070    | 2.46             | -0.31        | $0.78_{-0.03}^{+0.03}$           | 2                      | 4  |                      |   |  |
| 1229+204              | Ton 1542     | 0.064    | 2.63             | -0.59        | $1.5_{-0.1}^{+0.2}$              | 1                      | 2  | 45                   | 2   | 3170                                       |
| 1244+026              | PG           | 0.048    | 1.54             | -0.27        | $1.6_{-0.7}^{+0.7}$              | 1                      | 3, 6                                     |                      |   |  |
| 1304+346              | AB 133       | 0.189    | 0.50             | $\leq -0.58$ | $1.0_{-0.2}^{+0.6}$              | 5                      | 1  |                      |   |  |
| 1307+085              | PG           | 0.158    | 3.43             | -0.99        | $0.9_{-0.2}^{+0.2}$              | 1                      | 3, 6                                     | <8                   | 1   | 5570                                       |
| 1407+265              | PG           | 0.944    | 2.27             | 0.54         | $1.2_{-0.9}^{+0.9}$              | 1                      | 3  |                      |   |  |
| 1416-129              | PG           | 0.129    | 3.1              | 0.07         | $0.9_{-0.5}^{+0.2}$              | 1                      | 3  | <3                   | 1   | 4640                                       |
| 1426+015              | PG           | 0.086    | 3.66             | -0.48        | $1.2_{-0.2}^{+0.2}$              | 1                      | 3  | >20                  | 1   | 5540                                       |
| 1501+106              | Mkn 841      | 0.036    | 7.04             | -0.67        | $0.93_{-0.04}^{+0.04}$           | 1                      | 4  | 26*                  | 1   | 5360                                       |
| 1613+658              | Mkn 876      | 0.129    | 2.42             | 0.10         | $1.1_{-0.2}^{+0.2}$              | 1                      | 3  | 16                   | 1   | 7050                                       |
| 1803+676              | KAZ 102      | 0.136    | 1.70             | $\leq -0.69$ | $-0.2_{-0.3}^{+0.4}$             | 6                      | 3  | <0.2                 | 1, 2                                      | 4810                                       |
| 2130+099              | PG, IIZw 136 | 0.061    | 4.78             | -0.37        | $0.81_{-0.07}^{+0.07}$           | 1                      | 4  |                      |   |  |
| 2251-178              | MR           | 0.068    | 4.48             | -0.15        | $0.3_{-0.6}^{+0.5}$              | 7                      | 1  |                      |   |  |

<sup>a</sup>  $f_B$  is calculated from  $B$  using  $m_B(0) = 4440$  Jy (Johnson 1966). When  $B$ -magnitudes were not available,  $V$ -magnitudes were used.

<sup>b</sup> References for the radio flux density: (1) Kellermann et al. 1989; (2) Wilkes & Elvis 1987; (3) Condon et al. 1981; (4) Stocke et al. 1992; (5) Marshall 1987; (6) Hutchings & Gower 1985; (7) Ricker et al. 1978.

<sup>c</sup> References: (1) this paper; (2) Wilkes et al. 1987; (3) Wilkes & Elvis 1987; (4) Masnou et al. 1992; (5) Elvis et al. 1993; (6) Elvis et al. 1986.

<sup>d</sup> Equivalent width of Fe II  $\lambda 4570$  in the quasar's rest frame (uncertainties are  $\sim \pm 10\%$ ).

<sup>e</sup> Full width at half-maximum of H $\beta$  in the observed frame.

<sup>f</sup> Errors on  $\alpha_E$  are scaled to  $1 \sigma$  from the 90% errors given in Wilkes et al. 1987.

\* He II  $\lambda 4686$  excluded from measurement.

(1987) who took  $f_R$  to be the core radio flux density where available rather than the total value. The change of definition largely affects the values for RLQs. In Figure 1a we show the distribution of radio-loudness for the quasars in our sample. The distribution is clearly bimodal, consistent with what has been found for other samples of quasars (Kellermann et al. 1989; Stocke et al. 1992). A quasar is thus classified as "radio-loud" when  $\log(f_R/f_B) > 1$ .

In Tables 1 and 2, the updated soft X-ray energy indices are listed for the RQQs and RLQs, respectively. The distribu-

tions of the X-ray energy indices are shown in Figure 1b. The RLQs have stochastically flatter X-ray energy indices than the RQQs at a level greater than 99.95% as given by a Mann-Whitney  $U$ -test. This confirms the earlier result of Wilkes & Elvis (1987). The RQQ 1803+676 remains an exceptional object with an extremely flat ( $\approx -0.2$ ) slope.<sup>5</sup>

<sup>5</sup> The X-ray slope of 1803+676 was incorrectly listed as 0.2 in Table 3 of Wilkes & Elvis (1987).

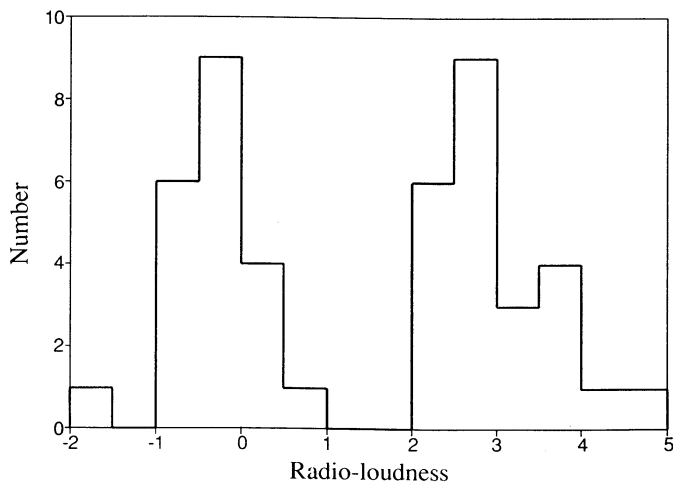


FIG. 1a

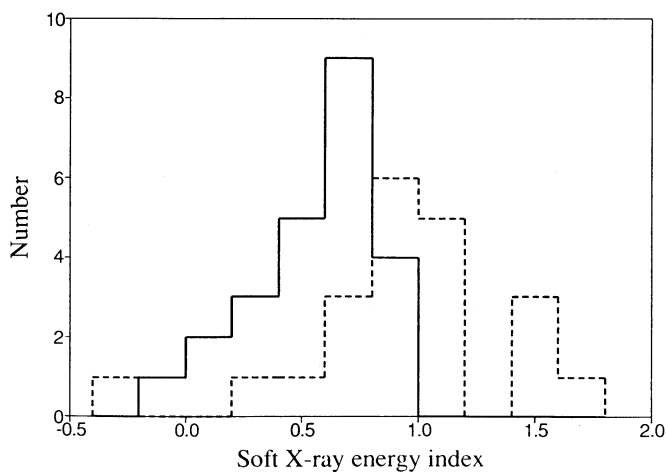


FIG. 1b

FIG. 1.—Distribution of the radio-loudness parameter ( $R_{L_i}$ ) for the quasars in our sample. (For the definition of radio-loudness see § 2.) (b) Distributions of soft X-ray energy index  $\alpha_E$  of the radio-loud (solid line) and radio-quiet (dashed line) quasars in our sample.

TABLE 2  
RADIO-LOUD QUASARS

| Source        | Other Name  | Redshift | $f_B^a$<br>(mJy) | $R_{Lr}$ | $R$  | $\alpha_E$<br>( $\pm 1 \sigma$ ) | References <sup>b</sup> | References <sup>c</sup><br>( $\alpha_E$ ) | $W_\lambda^d$<br>(Å) | References <sup>c</sup><br>( $W_\lambda$ ) | FWHM <sup>e</sup><br>(km s <sup>-1</sup> ) |
|---------------|-------------|----------|------------------|----------|------|----------------------------------|-------------------------|---|----------------------|--|--|
| 0007+106..... | III Zw 2    | 0.089    | 1.83             | 2.24     | 0.9  | $0.4^{+0.9}_{-0.3}$              | 1                       | 3   | 5                    | 2  | 4700                                       |
| 0133+207..... | 3C 47       | 0.425    | 0.24             | 3.65     | 0.07 | $0.9^{+0.3}_{-0.3}$              | 2                       | 3   |                      |  |  |
| 0134+329..... | 3C 48       | 0.367    | 1.40             | 3.61     | CSS  | $0.7^{+0.4}_{-0.4}$              | 3                       | 3   |                      |  |  |
| 0312-770..... | PKS         | 0.223    | 1.39             | 2.60     | 11   | $0.1^{+0.6}_{-0.2}$              | f                       | 3   | 18                   | 2  | 3340                                       |
| 0637-752..... | PKS         | 0.656    | 1.64             | 3.53     | >10  | $0.5^{+0.1}_{-0.1}$              | f                       | 4   |                      |  |  |
| 0837-120..... | 3C 206, PKS | 0.198    | 2.16             | 2.58     | 0.3  | $0.6^{+0.3}_{-0.3}$              | 4                       | 5   | <8                   | 1  | 4485                                       |
| 0903+169..... | 3C 215      | 0.411    | 0.18             | 3.36     | 0.05 | $0.0^{+0.6}_{-0.2}$              | 2                       | 3   |                      |  |  |
| 0923+392..... | 4C 39.25    | 0.699    | 0.30             | 4.39     | 36   | $0.4^{+0.1}_{-0.1}$              | 5                       | 3   |                      |  |  |
| 1020-103..... | PKS         | 0.197    | 1.40             | 2.44     | 5.5  | $0.8^{+0.7}_{-1.6}$              | 6                       | 1   |                      |  |  |
| 1028+313..... | B2          | 0.177    | 0.66             | 2.38     | 1.3  | $0.62^{+0.06}_{-0.06}$           | 7                       | 4   | <3                   | 1  | 4280                                       |
| 1100+772..... | 3C 249.1    | 0.311    | 2.33             | 2.52     | 0.1  | $1.0^{+0.3}_{-0.3}$              | 8                       | 3   |                      |  |  |
| 1111+408..... | 3C 254      | 0.734    | 0.25             | 3.50     | 0.02 | $1.0^{+0.5}_{-0.3}$              | 9                       | 1   |                      |  |  |
| 1128+315..... | B2          | 0.289    | 1.0              | 2.39     | 10   | $0.7^{+0.5}_{-0.5}$              | f                       | 1   |                      |  |  |
| 1137+660..... | 3C 263      | 0.656    | 1.12             | 2.97     | 0.2  | $0.7^{+0.4}_{-0.1}$              | 8                       | 3   |                      |  |  |
| 1146-037..... | PKS         | 0.341    | 0.73             | 2.37     | 1.4  | $0.3^{+0.3}_{-0.3}$              | 10                      | 3   | 3                    | 2  | 4300                                       |
| 1217+023..... | PKS         | 0.240    | 1.07             | 2.64     | 2.0  | $0.5^{+0.3}_{-0.1}$              | 6                       | 3   |                      |  |  |
| 1226+023..... | 3C 273      | 0.158    | 26.27            | 3.12     | 5.5  | $0.47^{+0.03}_{-0.03}$           | 5                       | 4   | 15                   | 1, 2                                       | 4300                                       |
| 1253-055..... | 3C 279      | 0.538    | 0.28             | 4.58     | 7.8  | $0.6^{+0.1}_{-0.3}$              | 5                       | 3   |                      |  |  |
| 1545+210..... | 3C 323.1    | 0.266    | 0.85             | 3.04     | 0.05 | $0.8^{+0.3}_{-0.5}$              | 2                       | 3, 6                                      |                      |  |  |
| 1635+119..... | MC          | 0.146    | 0.72             | 2.05     | 0.3  | $0.9^{+1.0}_{-1.0}$              | 7                       | 3   |                      |  |  |
| 1704+608..... | 3C 351      | 0.371    | 3.04             | 2.60     | 0.02 | $0.1^{+0.9}_{-0.5}$              | 4                       | 5   | 3 <sup>g</sup>       | 1  | 2420                                       |
| 1721+343..... | 4C 34.47    | 0.206    | 1.1              | 2.76     | 1.2  | $0.5^{+0.4}_{-0.3}$              | 11                      | 3   |                      |  |  |
| 2128-123..... | PKS         | 0.501    | 2.49             | 2.92     | >20  | $0.5^{+0.8}_{-0.3}$              | 12                      | 1   |                      |  |  |
| 2135-147..... | PKS         | 0.200    | 1.77             | 2.99     | 0.09 | $0.73^{+0.05}_{-0.05}$           | 12                      | 4   |                      |  |  |

<sup>a</sup>  $f_B$  is calculated from  $B$  using  $m_B(0) = 4440$  Jy (Johnson 1966). When  $B$ -magnitudes were not available,  $V$ -magnitudes were used.

<sup>b</sup> References for the core radio flux density: (1) Kellermann et al. 1989; (2) Swarup et al. 1984; (3) Pearson et al. 1985; (4) Antonucci & Barvainis 1988; (5) Perley et al. 1982; (6) Gower & Hutchings 1984; (7) Feigelson et al. 1984; (8) Wills et al. 1993; (9) Owen & Puschell 1984; (10) Hintzen et al. 1983; (11) Barthel et al. 1989; (12) Wills & Browne 1986.

<sup>c</sup> References: (1) this paper; (2) Wilkes et al. 1987; (3) Wilkes & Elvis 1987; (4) Masnou et al. 1992; (5) Elvis et al. 1993; (6) Elvis et al. 1986.

<sup>d</sup> Equivalent width of Fe II  $\lambda 4570$  in the quasar's rest frame (uncertainties are  $\sim \pm 10\%$ ).

<sup>e</sup> Full width at half-maximum of H $\beta$  in the observed frame.

<sup>f</sup>  $R_{cd}$  is estimated from the total radio spectral index between 2.7 and 5 GHz.

<sup>g</sup> He II  $\lambda 4686$  excluded from measurement.

A simple mean of the X-ray energy indices for the RQQs is  $1.0 \pm 0.1$ , in good agreement with the mostly overlapping sample of Wilkes & Elvis (1987), and with the higher energy (2–10 keV) indices determined from *EXOSAT* and *Ginga* for a similar sample of quasars (Comastri et al. 1992; Williams et al. 1992). A weighted mean is somewhat lower,  $0.85 \pm 0.02$ , due to the strong dominance of a small number of objects with well-determined energy indices. Notably, the quasar energy indices are systematically steeper than the high-energy indices seen in Seyfert 1 galaxies where reflection of X-rays from cool, optically thick gas gives a good fit to the data (Pounds et al. 1990; Williams et al. 1992).

In Figure 2 the radio-loudness parameter ( $R_{Lr}$ ) is plotted against the soft X-ray energy index. The systematic difference between RLQs and RQQs reported by Wilkes & Elvis (1987) is once again clear. The formal significance of a correlation between  $\alpha_E$  and  $R_{Lr}$  is greater than 99.95% although the distribution of the data now suggests two classes of objects rather than a real correlation. There is no significant correlation within the subsamples of RQQs or RLQs (less than 90% probability, Spearman Rank test), supporting the idea that they form two different populations (Miller, Peacock, & Mead, 1990; Smith & Heckman 1990; Williams et al. 1992; Stocke et al. 1992). The dichotomy is consistent with the suggestion that differing emission mechanisms dominate the X-ray emission in the two classes, as originally suggested by Zamorani et al. (1981).

As was pointed out by Wilkes & Elvis (1987), ignoring the statistical difference in  $\alpha_E$  between RQQs and RLQs while

estimating X-ray luminosities leads to an underestimate of the luminosities of RQQs relative to those of RLQs (Wilkes & Elvis 1987, Fig. 6), but a much larger difference would be required to attribute the difference in luminosities of the two classes (Zamorani et al. 1981; Worrall et al. 1987) to the difference in  $\alpha_E$  alone.

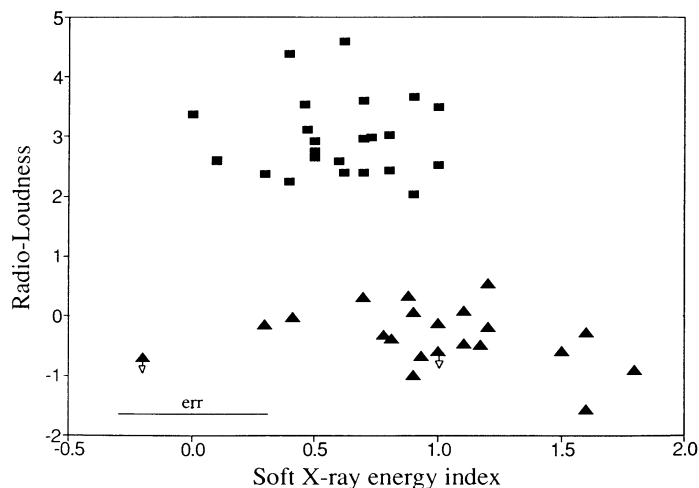


FIG. 2.—Radio-loudness parameter ( $R_{Lr}$ ) (§ 2) plotted against the soft X-ray energy index for the RLQs (filled squares) and RQQs (filled triangles) in the sample. The typical  $1 \sigma$  error in the X-ray energy index is shown.

### 3. X-RAY ENERGY INDICES AND RADIO CORE DOMINANCE

In the framework of the “unified interpretation” for RLQs (Blandford & Königl 1979), bulk relativistic motion is ubiquitous in them. The observed flux density of the nuclear component is then Doppler-boosted at small angles of the motion to the line-of-sight, and differences between radio core-dominated (CDQs) and lobe-dominated quasars (LDQs) are due to orientation alone. The core-dominance parameter,  $R_{cd}$ , defined as the ratio of the radio flux density from the nucleus to that from the radio lobes, is then a statistical measure of the angle of inclination of the nuclear jet to the line-of-sight (Kapahi & Saikia 1982; Orr & Browne 1982). Interpreting correlations of X-ray luminosity with nuclear and lobe radio luminosities in this framework, Browne & Murphy (1987) suggested that a component of the X-ray emission in RLQs is orientation-dependent.

The soft X-ray energy indices have been found to be systematically flatter for CDQs than for LDQs; (Canizares & White 1989; Boroson 1989; Shastri 1991). Based on this trend, Shastri (1991) suggested that the “radio-linked” component of the X-ray emission (Zamorani et al. 1981; Kembhavi, Feigelson, & Singh 1986; Wilkes & Elvis 1987) is probably relativistically beamed.

The values of the core-dominance parameter ( $R_{cd}$ ) for the RLQs in our sample (updated from Shastri 1991) are given in Table 2. They were determined at an observed frequency of 5 GHz (except 1146–037, for which the peak flux density of the core at 1.4 GHz was used, assuming a spectral index of 0). The core radio flux densities are from high-resolution radio images. If lobe flux densities were not available, they were derived from the total flux density. For three exceptions noted in Table 2,  $R_{cd}$  was estimated from the total radio spectral index, assuming spectral indices of 0 and 1 for the core and lobes, respectively.

Figure 3 shows that the X-ray energy index for our larger sample correlates inversely with  $\log R_{cd}$ , except for two quasars that are highly discrepant (see below). A Spearman rank test shows the correlation to be significant at the 99.95% level (one-tailed test) without the discrepant objects, and at the 90% level if they are included. Note that we have excluded the one compact steep-spectrum quasar in the sample (3C 48:

0134+329) from Figure 3, because, as is common in these objects, the core shows complex radio structure (Spencer et al. 1989; also Fanti et al. 1990) and interaction of the radio jet with the interstellar medium is believed to be significant (van Breugel, Miley, & Heckman 1984). The radio flux density of the nuclear components must reflect this interaction, in which case the parameter  $R_{cd}$  is not a good measure of orientation.

In the framework of the unified interpretation, the correlation in Figure 3 is either due to a flat-spectrum X-ray component dominating at face-on inclinations, or due to a steep-spectrum component dominating at edge-on inclinations. It certainly cannot be explained by the anisotropy of the steep “ultrasoft excess” (Wilkes & Elvis 1987); simple inclination effects for a thin disk would result in stronger ultrasoft emission at face-on orientations (assuming that the disk is perpendicular to the radio axis); relativistic effects could divert a significant amount of ultra-soft X-ray radiation from the inner parts of the disk to the equatorial observer (e.g., Cunningham 1975), but in any case the ultrasoft excess is observed at energies below 0.3 keV, and therefore cannot significantly affect the soft X-ray spectra (0.2–3.5 keV). On the other hand, as was argued in Shastri (1991), bulk relativistic motion of material emitting a flat-spectrum X-ray component, (such as the nuclear jet), would give the required anisotropy. This suggestion fits in with the picture of an additional, flat-spectrum X-ray component associated with the radio emission in RLQs (Zamorani et al. 1981; Kembhavi et al. 1986; Wilkes & Elvis 1987; also see model in Kembhavi, Wagh, & Narasimha 1989). X-ray emission from radio jets is not unknown. Burns, Feigelson, & Schreier (1983) find very good spatial coincidence of structures of the jet in the radio galaxy Centaurus A as observed in the radio and X-ray bands. Harris & Stern (1987) measure a position for the candidate X-ray jet feature in the quasar 3C 273 which is coincident with one of the optical jet features imaged by Fraix-Burnet & Nieto (1988) (the latter’s feature B). Similar coincidence is reported for knots in M87 (Biretta, Stern, & Harris 1991).

The above correlation with  $R_{cd}$  would contribute to the correlation of X-ray slope with core radio-loudness found by Wilkes & Elvis (1987), since it turns out that the core radio-loudness is correlated with  $R_{cd}$  for the RLQs in the sample.

The correlation in Figure 3 is consistent with the inhomogeneous jet model of Ghisellini, Maraschi, & Treves (1985), proposed for the nonthermal emission from BL Lacertae-type objects (also see Maraschi 1992). The model proposes two components of X-ray emission from the jet; the first is a synchrotron component from close to the nucleus which has a steep spectrum, and is relativistically beamed but into a relatively wide angle. The second is an inverse Compton component from the outer regions of the jet, that has a flat spectrum and is beamed into a cone narrower than that of the first component, either because of higher bulk velocities or greater collimation in the outer regions of the jet. Thus the model predicts that the compound X-ray spectrum will flatten as orientation changes from more edge-on to face-on inclinations of the nuclear jet. In the unified scheme, this would translate to flattening of the observed X-ray spectrum with increase of radio core dominance, as seen in Figure 3.

The trend in Figure 3 is inconsistent with the scenario of Melia & Königl (1989) within the unified scheme. In the context of explaining BL Lacertae-type objects they proposed that the hard X-ray component is due to the inverse Compton “drag” on the relativistic jet by thermal radiation from the

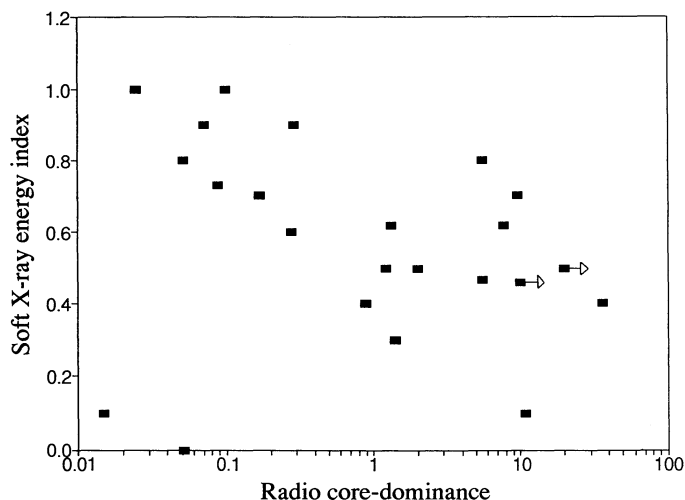


FIG. 3.—For the RLQs, the soft X-ray energy index  $\alpha_E$  is plotted against the logarithm of the radio core-dominance parameter  $R_{cd}$  (§ 3).

nuclear disk near the nucleus, and the steep-spectrum component is direct synchrotron emission from further out in the jet. The hard component is more isotropic than the steep spectrum component. It follows that the steep spectrum component would then dominate at face-on orientations, and the unified scheme would predict that the steep X-ray component dominate at large  $R_{cd}$ -values, opposite to that seen in Figure 3.

Tests in the framework of the unified interpretation are most meaningful when the RLQs are chosen to have a narrow spread in an orientation-independent parameter. A study to test the above result with a sample of RLQs matched with respect to their radio lobe luminosities is underway with *ROSAT*. We note, however, that no trend of X-ray slope with radio lobe luminosity is indicated for the present sample.

It is suggestive that two of the quasars with amongst the lowest  $R_{cd}$ -values have nominally flat X-ray energy indices (although with large uncertainties). We speculate that at the most edge-on inclinations of the quasar the steep-spectrum X-ray component may be occulted (by an obscuring torus?), leaving the residual flat-spectrum component that originates from further out in the jet still visible.

#### 4. X-RAY ENERGY INDICES AND THE OPTICAL Fe II EMISSION

The well-known but unexplained inverse relation between radio emission and optical Fe II strength (Peterson, Foltz, & Byard 1981; Phillips 1977; Boroson & Green 1992) was suggested by Wilkes, Elvis, & McHardy (1987) to be a secondary relation caused by correlations between the equivalent width of the Fe II  $\lambda 4570$  emission-line strength and the soft X-ray energy index  $\alpha_E$  (based on a sample of nine quasars) and between  $\alpha_E$  and radio loudness. This was later disputed, however, by Boroson (1989) and Zheng & O'Brien (1990), after finding no correlation for samples of 15 and 33 quasars respectively. Boroson (1989) claimed that the inconsistency with Wilkes, Elvis, & McHardy (1987) was due to a combination of the samples being different and the measurements being inconsistent, while Zheng & O'Brien (1990) claimed that it was their equivalent width measurements of three additional quasars that destroyed the correlation.

In Tables 1 and 2 we present Fe II  $\lambda 4570$  equivalent widths for 18 of the present sample of quasars. Previously unpublished optical spectrophotometry was obtained with the Faint Object Grism Spectrograph on the Multiple Mirror Telescope on 1988 April 8–9. Each quasar was observed through a  $10'' \times 30''$  slit to obtain accurate spectrophotometry and through a narrow ( $1''.25$ ) long slit for 5–15 minutes to yield improved spectral resolution ( $\sim 8 \text{ \AA}$ ) and signal-to-noise. The large-aperture spectra were flux calibrated with reference to a nearby standard star and then the small aperture spectra were normalized to the same flux level. All the observations were made under photometric conditions, and at air masses  $\lesssim 1.4$ . The spectral region surrounding the Fe II  $\lambda 4570$  feature for each of these quasars is displayed in Figures 4a and 4b.

The difficulty of measuring Fe II emission line strengths (due to their extreme blending) is well known and frequently results in discrepant measurements. To minimize such problems our sample was confined to objects for which our spectra could be measured in a uniform and straightforward manner. The strength of the Fe II  $\lambda 4570$  blend was measured above a linear baseline extending between the continuum regions immediately longward of H $\gamma$   $\lambda 4340$  and shortward of H $\beta$   $\lambda 4861$ . This is a very simple measurement, staying as close as possible to

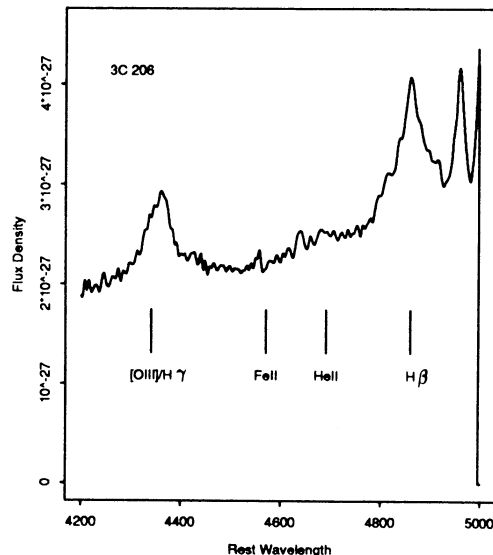


FIG. 4.—(a) Optical spectrophotometry of 0837–120 showing the Fe II  $\lambda 4570$  features, with the different spectral features labeled. (b) Optical spectrophotometry of the rest of the RQs and RLQs, ordered in right ascension, showing the Fe II features whose measurements are given in Tables 1 and 2.

the data and not subject to any underlying assumptions. This contrasts with the global fitting method of Boroson & Green (1992) for example which, while superior in some ways, requires that the ratios between multiplets remain fixed. A comparison of these two samples is made below. Since for large emission-line widths the continuum level is likely to be overestimated due to blending of the hydrogen line wings into those of the Fe II emission (Wills 1988), we include only quasars with lines narrower than  $6000 \text{ km s}^{-1}$  (with the exception of PG 1613+658 where the continuum level is clear despite the large FWHM of  $7050 \text{ km s}^{-1}$ ). We point out that while our method of determination of the equivalent widths is a simple one and may not give accurate absolute values, it yields meaningful relative values within our sample. The He II  $\lambda 4686$  emission line is included in this measurement unless noted, since deblending is highly inaccurate for such heavily blended lines. He II is a high-ionization line, probably from different gas than the Fe II lines, and thus its inclusion is only likely to add scatter into any relation followed by the Fe II emission. The rest frame equivalent widths as derived from our measurements are listed in Table 1 for the RQs and Table 2 for the RLQs.

Figure 5a shows the Fe II equivalent width plotted against the soft X-ray energy index. RQs, CDQs ( $R_{cd} > 0.5$ ) and LDQs ( $R_{cd} \leq 0.5$ ) are marked separately. The correlation between Fe II strength and  $\alpha_E$  is significant at the 99% level (Spearman rank test) for the full sample or for RQs alone, although it is clear from the figure that the RLQs show no trend. PG 1416–129 has a very flat X-ray energy index in *Ginga* observations ( $0.05 \pm 0.15$ , Williams et al. 1992). Given the poor constraints on the *Einstein* value ( $0.9 \pm 0.5$ , 68% confidence range), the two results are consistent (the difference being less than  $2 \sigma$ ). If the *Ginga* value is used in preference (indicated by a filled square in Fig. 5a), the correlation is further strengthened (significance greater than 99.5%).

Although, as noted above, the full range of FWHM is not included here to avoid measurement problems, we note that no correlation between  $\alpha_E$  and H $\beta$  FWHM is seen in the current

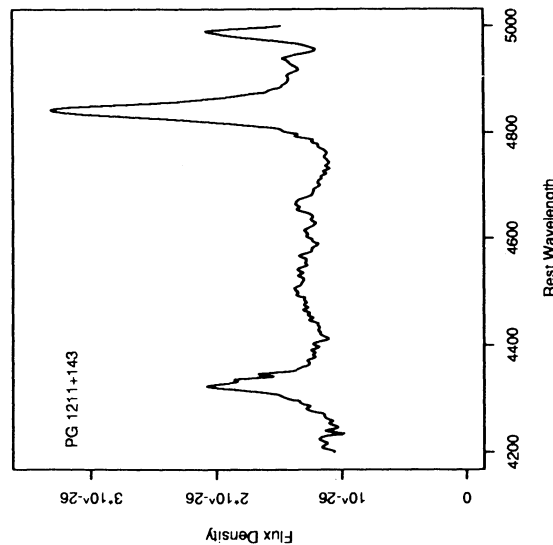
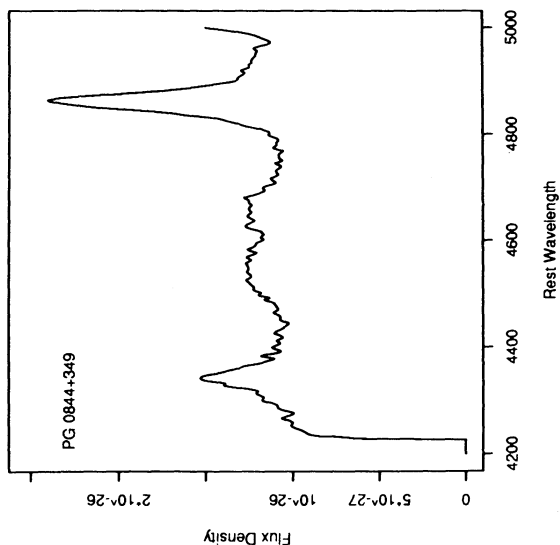
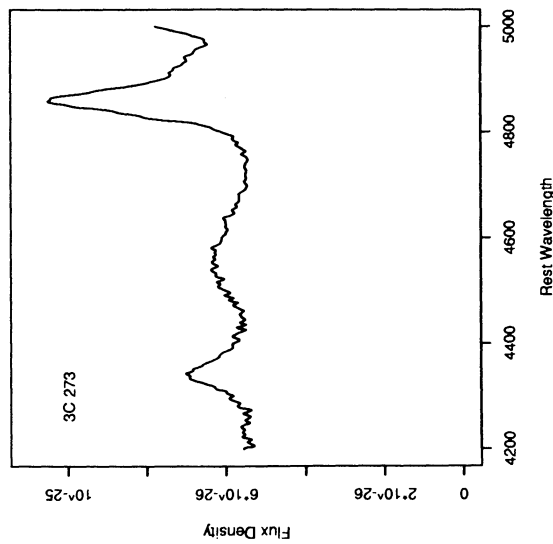
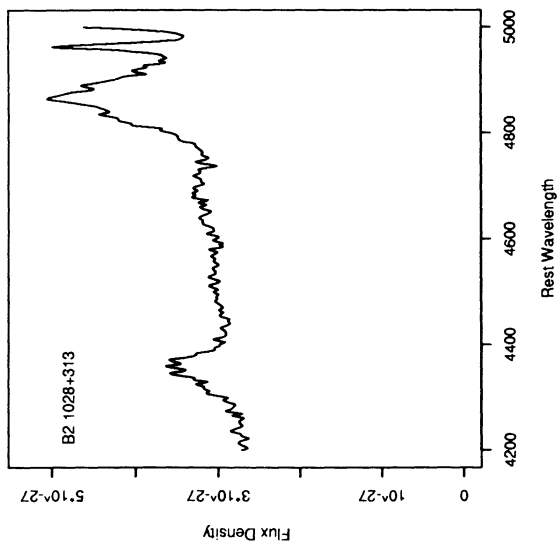
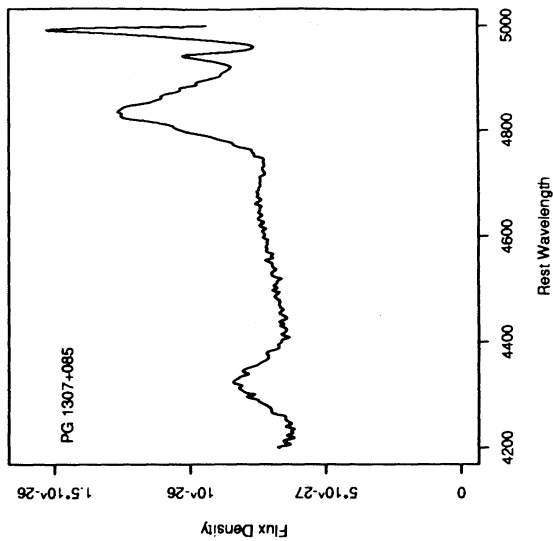
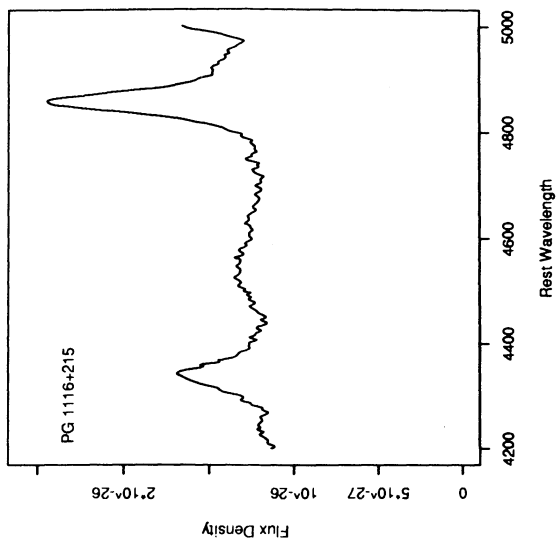


FIG. 4b

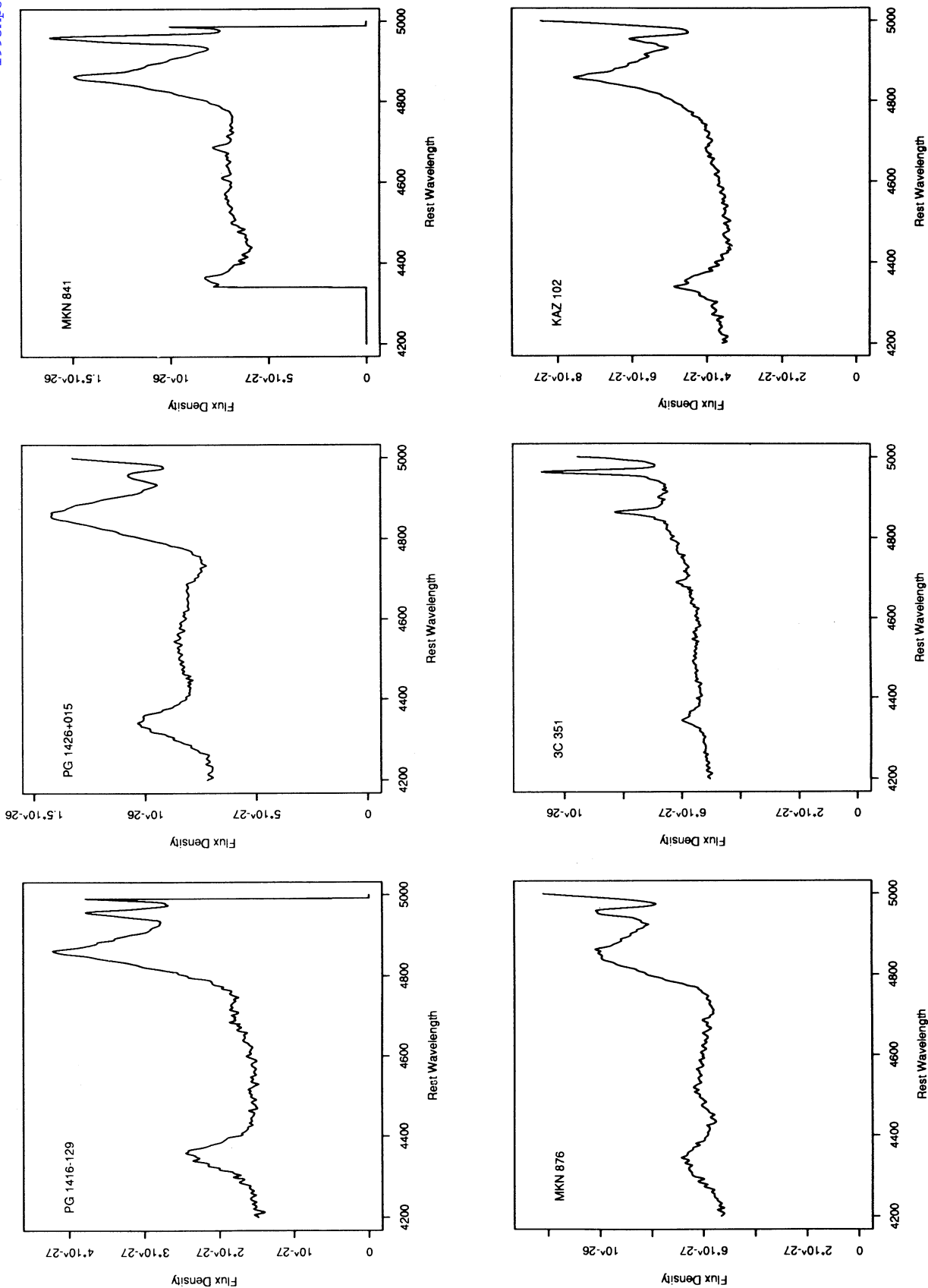


FIG. 4b—Continued

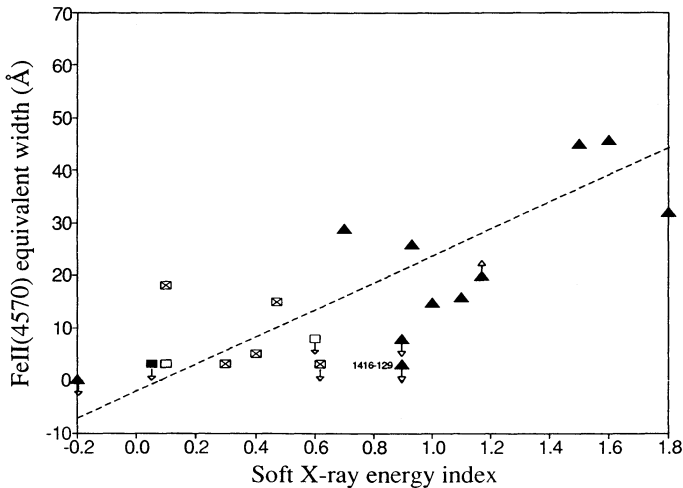


FIG. 5a

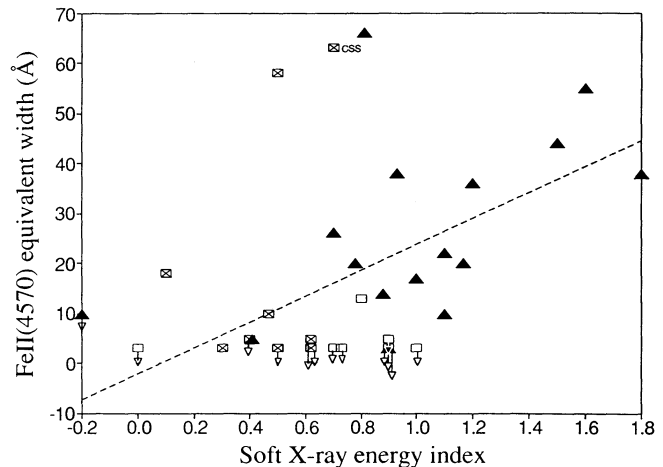


FIG. 5b

FIG. 5.—(a) Rest frame equivalent width of the Fe II  $\lambda 4570$  multiplet plotted against the soft X-ray energy index  $\alpha_E$ . Separately shown are RQQs (filled triangles), CDQs (crossed squares) and LDQs (empty squares). The single filled square is the *Ginga* measurement for 1416–129, whose IPC measurement has large errors. The dashed line represents a simple regression on the RQQ data to allow comparison with Fig. 5b (b) Same plot as in Fig. 5a but for the data from Zheng & O'Brien (1990). The symbols are as in Fig. 5a. The compact steep spectrum (CSS) object is 0134 + 329 (3C 48). The regression line from Fig. 5a is shown for comparison.

sample. Thus our exclusion of quasars with very broadened lines cannot spuriously give rise to the correlation in Fig. 5a.

The same plot as above with Fe II  $\lambda 4570$  equivalent width data from Zheng & O'Brien (1990) is shown in Figure 5b. There is no significant correlation for the sample as a whole (as indeed is asserted by the authors), nor for the RLQs, but the RQQs show a trend similar to Figure 5a (significance greater than 95%). There appear to be no major inconsistencies between their measurements and estimation procedure and ours. However, there remains one highly discrepant RQQ, 2130+099 (also in the sample of Boroson 1989, but not in our sample) which has strong Fe II emission but an intermediate soft X-ray slope ( $\alpha_E = 0.8$ ).

The data of Boroson (1989) do not show a correlation even for the RQQs. He uses the equivalent width of a different Fe II multiplet ( $\lambda\lambda 5105\text{--}5395$ ), but shows a tight correlation between the Fe II  $\lambda\lambda 5105\text{--}5395$  and Fe II  $\lambda\lambda 4500\text{--}4680$  equivalent widths. Fourteen of Boroson's objects have data in either Zheng & O'Brien (1990) or in Tables 1, 2, or both. Of these, for seven objects, the equivalent width measurements are consistent with the present measurements and/or those of Zheng & O'Brien (1990); for the remaining seven, however, (including four RQQs), the equivalent widths of Boroson (1989) are highly discrepant. The reasons for this discrepancy are unclear.

While the high-energy X-ray energy indices (2–10 keV) determined by *Ginga* do not by themselves show any significant correlation with the Fe II equivalent width (Williams et al. 1992), the data for RQQs (available for five objects) are broadly consistent with Figure 5a.

Recently Boroson & Green (1992) have published equivalent widths of the Fe II multiplet for quasars of low redshift from the BQS catalog. The empirical technique that they use allows an estimate of equivalent widths that is independent of the line width. A comparison of the 12 quasars in common with our Fe II sample shows that their measurements are systematically higher, possibly due to our overestimating the continuum despite our exclusion of lines broader than  $6000 \text{ km s}^{-1}$ . However, for three of the objects (1116+215, 1226+023 and 1613+658) the values are grossly inconsistent, although the spectra look similar to ours. This comparison reinforces our decision not to combine different samples. However, if we look

at the objects from Boroson & Green (1992) alone, despite the small range of Fe II equivalent widths present, the data for 14 quasars for which we have X-ray energy indices are consistent with the trend seen in Figure 5a (though with systematically higher values of Fe II emission strength), and the correlation of  $\alpha_E$  with Fe II equivalent width is significant at a greater than 90% level if the *Ginga* value of  $\alpha_E$  for 1416–129 is used.

Standard photoionization models for the line emission from the broad-line regions of quasars (Krolik 1988) imply a close link between the energy index of the ionizing X-ray continuum and the strength of the Fe emission lines. In the case of the RLQs, however, if the soft X-ray emission has a significant contribution from the radio jet as has been discussed above, then the X-ray energy index would not be a good indicator of the spectrum of the ionizing continuum. The absence of a correlation between the line strengths and the X-ray slope for RLQs is therefore not necessarily surprising. Joly (1991) has claimed a significant correlation of  $R_{\text{cd}}$  with Fe II equivalent widths in RLQs which cannot be fully explained by the broader lines in LDQs, but there are too few objects in our sample to test this.

Although we see a correlation of  $\alpha_E$  with Fe II strength for the RQQs, it is in the opposite sense to that predicted by the standard model in which the Fe II emission is generated deep within the cloud and thus is sensitive to harder X-rays. It should be kept in mind though, that the standard models fail to predict the large strength of the optical Fe II emission lines. Zheng & O'Brien (1990) find a strong relation between the strength of the optical Fe II emission and the H $\beta$  FWHM, which they conclude cannot be explained by overestimation of the continuum alone. They suggest that the geometry of the emitting regions may also play a role in determining the observed Fe II equivalent widths as discussed by Netzer, Laor, & Gondhalekar (1992) and references therein. It is possible that geometry plays a role in the observed X-ray energy index as well, just as it appears to do in the RLQs.

##### 5. THE RANGE OF X-RAY ENERGY INDICES

The existence of correlations of the X-ray energy index with external parameters in both the radio-quiet and radio-loud



subsamples allows us to strengthen the significance of the IPC measurements.

In the case of the RQQs the equivalent widths of the Fe II lines are entirely independent of the X-ray measurement so the correlation of Figure 5a can exist only if the soft X-ray energy indices have a real intrinsic range from  $\sim 0$  to  $\sim 1.5$ . This truly is a large range. It is, for example,  $\pm 4 \sigma$  either side of the *HEAO 2/EXOSAT* mean, given the dispersion measured in those samples (Petre et al. 1984; Turner & Pounds 1989). Since our sample is small and incomplete, we cannot determine the real distribution of the energy indices; the extremes we observe, however, cannot be rare.

Some active galactic nuclei (AGNs) have been discovered with the optical spectrum completely dominated by Fe II emission (Lawrence et al. 1988). Soft X-ray observations of these AGNs will test the Fe II/soft-X-ray-slope relation in extremis, and may uncover some of the softest AGNs. The alternative possibility is to measure Fe II strengths in AGNs selected to have particularly soft spectra, e.g., those from the "ultrasoft survey" (Cordova et al. 1992).

For the radio-loud sample a slightly smaller range of soft X-ray energy index is required,  $\sim 0-1$ , to produce the observed correlation of X-ray slope and core dominance. This correlation is immediately subject to interpretation in the beaming hypothesis, as discussed above.

A wide spread of soft X-ray energy indices for RQQs and RLQs is clearly required by their correlation with extrinsic parameters which themselves show extended ranges. For the RQQs, this implies the existence of (at least) another variable which affects their X-ray properties. This variable is at present unknown.

## 6. CONCLUSIONS

Using updated soft X-ray energy indices for a sample of 45 quasars, we conclude the following:

1. The trend that radio-loud quasars have systematically flatter power-law fits to the soft X-ray spectrum than radio-quiet quasars is confirmed.

2. The lack of a significant trend when each class is considered separately implies that radio-loud and radio-quiet quasars belong to two separate populations.

3. For the radio-quiet quasars, soft (0.2–3.5 keV) X-ray energy indices are consistent with those at higher (2–10 keV) energies but steeper than the high energy indices of Seyfert 1 galaxies where reflection of the X-rays gives a good fit to the data.

4. For the radio-loud quasars, X-ray energy index correlates with the radio core-dominance. Within the framework of the unified interpretation this result suggests that a flat-spectrum X-ray component dominates due to Doppler enhancement when the quasar jet is pointed towards us.

5. A significant correlation exists between the Fe II optical emission line strengths and X-ray energy index for the 11 radio-quiet quasars from our sample. Radio-loud quasars do not follow the correlation, consistent with the predominance of an extra X-ray component associated with the radio jet. The correlation demonstrates a close observational link between quasar emission lines and the observed X-ray continuum which is thought to excite them. However, most current photo-ionization models predict a correlation in the opposite sense, with the Fe II emission generated deep inside the emitting clouds where only harder X-rays penetrate.

6. The fact that the soft X-ray energy indices correlate with independent properties (core-dominance for RLQs and Fe II equivalent widths for RQQs) argues for the wide range in the X-ray energy indices of both classes being real.

The authors would like to thank Beverley J. Wills and John T. Stocke for their critical comments. P.S. acknowledges support from the NSF grant AST-8714937 and NASA grant NAG 5-1700. M.E., B.J.W., and J.M. acknowledge support of the NASA grant NAGW 5-2201 (SARP) and contracts NAS 8-30751 (*HEAO 2*) and NAS 5-30934 (RSDC).

## REFERENCES

- Antonucci, R. R. J., & Barvainis, R. 1988, *ApJ*, 325, L21  
 Arnaud, K. A., et al. 1985, *MNRAS*, 217, 105  
 Barthel, P. D., Hooimeyer, J. R., Schilizzi, R. T., Miley, G. K., & Preuss, E. 1989, *ApJ*, 336, 601  
 Biretta, J. A., Stern, C. P., & Harris, D. E. 1991, *AJ*, 101, 1632  
 Blandford, R. D., & Königl, A. 1979, *ApJ*, 232, 34  
 Boroson, T. A. 1989, *ApJ*, 343, L9  
 Boroson, T. A., & Green, R. F. 1992, *ApJS*, 80, 109  
 Browne, I. W. A., & Murphy, D. W. 1987, *MNRAS*, 226, 601  
 Burns, J. O., Feigelson, E. D., & Schreier, E. J. 1983, *ApJ*, 273, 128  
 Canizares, C. R., & White, J. L. 1989, *ApJ*, 339, 27  
 Comastri, A., Setti, G., Zamorani, G., Elvis, M., Giommi, P., Wilkes, B. J., & McDowell, J. C. 1992, *ApJ*, 384, 62  
 Condon, J. J., O'Dell, S. L., Puschell, J. J., & Stein, W. A. 1981, *ApJ*, 246, 624  
 Cordova, F. A., Kartje, J. F., Thompson, R. J., Mason, K. O., Puchnarewicz, E. M., & Harnden, F. R. 1992, *ApJS*, 81, 661  
 Cunningham, C. T. 1975, *ApJ*, 202, 788  
 Elvis, M., Green, R. F., Bechtold, J., Schmidt, M., Neugebauer, G., Soifer, B. T., Matthews, K., & Fabbiano, G. 1986, *ApJ*, 310, 291  
 Elvis, M., et al. 1993, in preparation  
 Fanti, R., Fanti, C., Schilizzi, R. T., Spencer, R. E., Nan Rendong, Parma, P., van Breugel, W. J. M., & Venturi, T. 1990, *A&A*, 231, 333  
 Feigelson, E. D., Isobe, T., & Kembhavi, A. 1984, *AJ*, 89, 1464  
 Fraix-Burnet, D., & Nieto, J.-L. 1988, *A&A*, 198, 87  
 Ghisellini, G., Maraschi, L., & Treves, A. 1985, *A&A*, 146, 204  
 Gower, A. C., & Hutchings, J. B. 1984, *AJ*, 89, 1658  
 Harris, D. E., & Stern, C. P. 1987, *ApJ*, 313, 136  
 Hewitt, A., & Burbidge, G. 1987, *ApJS*, 63, 1  
 Hintzen, P., Ulvestad, J., & Owen, F. 1983, *AJ*, 88, 709  
 Hutchings, J. B., & Gower, A. C. 1985, *AJ*, 90, 405  
 Johnson, H. L. 1966, *ARA&A*, 4, 193  
 Joly, M. 1991, *A&A*, 242, 49  
 Kapahi, V. K., & Saikia, D. J. 1982, *J. Astrophys. Astron.*, 3, 465  
 Kellermann, K. I., Sramek, R., Schmidt, M., Shaffer, D. B., & Green, R. 1989, *AJ*, 98, 1195  
 Kembhavi, A., Feigelson, E. D., & Singh, K. P. 1986, *MNRAS*, 220, 51  
 Kembhavi, A., Wagh, S., & Narasimha, D. 1989, in *Active Galactic Nuclei*, ed. D. E. Osterbrock & J. S. Miller (Dordrecht: Kluwer), 209  
 Krolik, J. H. 1988, in *Supermassive Black Holes*, ed. M. Kafatos (Cambridge: Cambridge Univ. Press), 279  
 Kühr, H., Nauber, U., Pauliny-Toth, I. I. K., & Witzel, A. 1979, *Max-Planck Institut für Radioastronomie Preprint* 55  
 Lawrence, A., Saunders, W., Rowan-Robinson, M., Crawford, J., Ellis, R. S., Frenk, C. S., Efstathiou, G., & Kaiser, N. 1988, *MNRAS*, 235, 261  
 Maraschi, L. 1992, in *Variability of Blazars*, ed. E. Valtaoja & M. Valtonen (Cambridge: Cambridge Univ. Press), 447  
 Marshall, H. 1987, *ApJ*, 316, 84  
 Masnou, J.-L., Wilkes, B. J., Elvis, M., McDowell, J. C., & Arnaud, K. A. 1992, *A&A*, 253, 35  
 Melia, F., & Königl, A. 1989, in *BL Lac Objects*, ed. L. Maraschi, T. Macca-caro, & M.-H. Ulrich (Berlin: Springer), 372  
 Miller, L., Peacock, J. A., & Mead, A. R. G. 1990, *MNRAS*, 244, 207  
 Mushotzky, R. F. 1984, *Adv. Space Res.*, 3, 157  
 Orr, M. J. L., & Browne, I. W. A. 1982, *MNRAS*, 200, 1067  
 Owen, F. N., & Puschell, J. J. 1984, *AJ*, 89, 932  
 Netzer, H., Laor, A., & Gondhalekar, P. M. 1992, *MNRAS*, 254, 15  
 Pearson, T. J., Perley, R. A., & Readhead, A. C. S. 1985, *AJ*, 90, 738  
 Perley, R. A., Fomalont, E. B., & Johnston, K. J. 1982, *ApJ*, 255, L93  
 Peterson, B. A., Foltz, C. B., & Byard, P. L. 1981, *ApJ*, 251, 4  
 Petre, R., Mushotzky, R. F., Krolik, J. H., & Holt, S. S. 1984, *ApJ*, 280, 499

- Phillips, M. M. 1977, ApJ, 215, 746  
Pounds, K. A., Nandra, K., Stewart, G. C., George, I. M., & Fabian, A. C. 1990, Nature, 344, 132  
Ricker, G. R., Clarke, G. W., Doxsey, R. E., Dower, R. G., & Jernigan, J. G. 1978, Nature, 271, 35  
Shastri, P. 1991, MNRAS, 249, 640  
Smith, E. P., & Heckman, T. M. 1990, ApJ, 348, 38  
Spencer, R. E., McDowell, J. C., Charlesworth, M., Fanti, C., Parma, P., & Peacock, J. A. 1989, MNRAS, 240, 657  
Stoche, J. T., Morris, S. L., Weymann, R. J., & Foltz, C. B. 1992, ApJ, 396, 487  
Swarup, G., Sinha, R. P., & Hilldrup, K. 1984, MNRAS, 208, 813  
Turner, T. J., & Pounds, K. A. 1989, MNRAS, 240, 833  
van Breugel, W., Miley, G., & Heckman, T. M. 1984, AJ, 89, 5  
Veron-Cetty, M.-P., & Veron, P. 1991, ESO Sci. Rep. 10  
Wilkes, B. J., & Elvis, M. 1987, ApJ, 323, 243  
Wilkes, B. J., Elvis, M., & McHardy, I. 1987, ApJ, 321, L23  
Williams, O. R., et al. 1992, ApJ, 389, 157  
Wills, B. J. 1988, in Physics of Formation of Fe II Lines Outside LTE, ed. R. Viotti, A. Vittani, & M. Freidjung (Dordrecht: Reidel), 161  
Wills, B. J., et al. 1993, in preparation  
Wills, B. J., & Browne, I. W. A. 1986, ApJ, 302, 56  
Worrall, D. M., Giommi, P., Tananbaum, H., & Zamorani, G. 1987, ApJ, 313, 596  
Zamorani, G., et al. 1981, ApJ, 245, 357  
Zheng, W., & O'Brien, P. T. 1990, ApJ, 353, 433

*Note added in proof.*—We have discovered an error in the X-ray energy index we used for 1704 + 608 and listed in Table 2; the correct value should be 0.3 (+0.5, -0.4). This represents a 0.4  $\sigma$  change and does not alter any of the conclusions in the paper.